AIAA JOURNAL
Vol. 44, No. 10, October 2006

Optical Observation of the Impingements of Nitrogen Tetroxide/Monomethylhydrazine Simulants

Tony Yuan,* Cetera Chen,† and Berlin Huang‡
National Cheng-Kung University, Tainan 70101, Taiwan, Republic of China

DOI: 10.2514/1.18375

The spray phenomena of doublet and triplet impingements of nitrogen tetroxide (NTO) and monomethylhydrazine (MMH) simulants were studied by the planar laser induced fluorescence technique. The total flow rates of the simulants were controlled at ∼8.00 g/s to simulate the operations of a 5-lb$_f$ rocket, and the ratios of the mass flow rates (O/F) of NTO and MMH simulants were varied from 1.0 to 2.4. Statistical analysis was employed to examine the probability distributions of the mass of individual simulants at 10 mm downstream from the impinging point. The distributions of local mixture ratios and flame temperatures were deduced, and the estimation of characteristic exhaust velocity was performed. The results revealed that the breakup and mixing of the impinging jets were closely related to the momentum flux ratio of the jets and the surface tension of the liquids. The triplet impingement was superior in symmetry and uniformity of the spray than that of the doublet impingement, and its mixing was less sensitive to the momentum flux ratio and showed a better mixing effect than doublet impingement at higher O/F ratio conditions. With the detailed distribution information provided by the optical technique, the optimum $\bar{C}^*$ occurred at $O/F = 1.18$ with doublet impingements for the operation of a 5-lb$_f$ NTO/MMH rocket.

Nomenclature

$\bar{C}^*$	=	average characteristic exhaust velocity
C_f	=	collective coefficient
$C^*_{x,y}$	=	local characteristic exhaust velocity
E_m	=	mixing efficiency
$f_{x,y}$	=	fluorescent intensity
$I_0(x, y)$	=	local intensity of incident light
k	=	ratio of specific heat
$\bar{M}$	=	average molecular weight
$\dot{m}$	=	mass flow rate ratio
$m_{x,y}$	=	local density of the simulant containing dye
n	=	number density of dye
O/F	=	mass flow rate ratio of oxidizer (NTO) and fuel (MMH)
P.I.	=	spray patternation index
$P_{x,y}$	=	local probability of mass
R	=	mixture ratio expressed as oxidizer mass divided by total mass
$R_{x,y}$	=	local mixture ratio expressed as local oxidizer mass divided by local fuel mass
$r_{\mathrm{sa}_{x,y}}$	=	local mixture ratio which is above R
$r_{\mathrm{sb}_{x,y}}$	=	local mixture ratio which is below R
$\bar{T}$	=	average exhaust temperature
$T_{x,y}$	=	local adiabatic flame temperatures

I. Introduction

THE applications of low-thrust nitrogen tetroxide/monomethylhydrazine (NTO/MMH) bipropellant thrusters are mainly on the reaction control of missiles and satellites for its storable, hypergolic, and superior specific-impulse characteristics compared to monosystems. The impinging combustion of NTO/MMH follows the conventional spray combustion pattern since droplets had been observed experimentally in the downstream of the burning spray [1]. Thus, the autoignition and combustion processes occur in the gas phase [2], and jets' impingement provides the energy and momentum required for atomization and mixing.

It is obvious that the mixing of the propellants is crucial for the performance of NTO/MMH thrusters. Factors such as momentum flux of the impinging jets, physical properties of fluids, and types of injectors may alter the distribution of liquid mass significantly. Conventionally, the mass distributions of sprays were analyzed by using a mechanical patternator. Rupe [3,4] investigated the mixing of doublet impinging jets and defined the optimum mixing condition from the calculation of the mixing efficiency. He proposed that the momentum and the diameter of the impinging jets must be equal to acquire the optimum uniformity and mixing characteristics. The same conclusions were made in the observations of doublet and split triplet impingements made by Won et al. [5]. Riebling [6] extensively reviewed the mixing data in the literature and deduced a correlation of area ratio, density ratio, and mixture ratio to the optimum mixing efficiency. In his correlation, the mixture ratio is still the most significant factor to the mixing efficiency. The mixing mechanism proposed by Ashgriz et al. [7] showed that the transmission of the momentum of the impinging jets influences the mixing of the liquids before atomizing. When the liquid jets disintegrated into droplets, the turbulent dispersion would improve the mixing in the spray. McHale et al. [8] studied the mixing of the doublet impingements with different geometry of the injector orifice. They concluded that the injector with the noncircular orifice can achieve the spray with superior mixing over that of the conventional circular orifice. For the multipair of doublet impinging research, the parameters such as the numbers of injector elements, the length of the chamber, the cant angle, and the fan spacing distance of the spray all have significant influence on the mixing efficiency of the impinging spray [9].

The spatial resolution of the mechanical patternator is characterized by the spatial density of the collecting grid. For the applications on the observation of the mass distribution in a small area, such as the observation near the injector tip, the mechanical patternator would be less adequate. Optical techniques, however, provide high-resolution, nonintrusive, and quantitative measurements of the spray. The planar laser induced fluorescence (PLIF) technique adopted by Jung et al. [10,11] was used to observe the mass distribution of droplets in various impinging sprays. Their optical measurements were justified by comparing to those from a mechanical patternator. A similar technique was used to observe the effects of the jet's momentum and surface tension on mass

Received 24 June 2005; accepted for publication 13 April 2006.

*Associate Professor, Department of Aeronautics and Astronautics, #1, Da Shia Road; yahn@mail.ncku.edu.tw.
†Graduate Student, Department of Aeronautics and Astronautics.
‡Graduate Student, Department of Aeronautics and Astronautics.

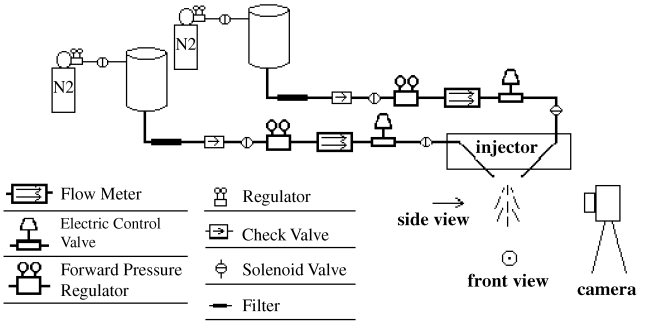

Fig. 1 The experimental setup.

distribution in unlike-doublet impinging sprays [12]. Both of them showed positive effects on fluid atomization as well as spray uniformity. By ratioing the fluorescent signals and the scattering signals of droplets in sprays, the Sauter mean diameter (SMD) distribution can be also deduced with careful calibration [13].

The phenomena and controlling factors of impinging sprays have been extensively studied, however, practical design information is scarce. This research focused on the design parameters of a 5–lb$_f$ NTO/MMH thruster. By using the simulants, this research observed the detailed mass distribution of individual propellant in the spray with the PLIF technique for both doublet- and triplet-impinging arrangements. Experiments were set for different mass flow rate ratios of NTO and MMH to simulate the actual thruster operations. Mixture ratio and temperature distributions were deduced from the mass distribution data. Mixing efficiency and characteristic exhaust velocity at various conditions were also analyzed.

II. Experimental Method

A nitrogen-compressing fluid supply system was used in this study (Fig. 1). The injector's orifices were 0.3 mm ID (inner diameter) ($L/d \approx 5$) and made of stainless steel. The impinging jets were oriented to have a $+30$ deg $/ -30$ deg angle. Water- and chloroform-based solutions were used as simulants to match the density, viscosity, and surface tension of MMH and NTO, respectively. The two simulants are immiscible and the physical properties of the simulants are listed in Table 1. From the previous study of unlike-doublet impingements, spray fan shifting and unevenly distributing of droplets were shown when the momentum flux ratio of the two jets departed from 1 [12]. Triplet impingement, another type of injector design which is commonly used in MMH/NTO rockets, however, can improve the above shortcoming. To control a constant total flow rate of $\sim$8 g/s to meet the operation specification of a 5-lb$_f$ MMH/NTO thruster, both doublet and triplet experiments were performed in this study. In practical, the propellant flow rates usually control at the mass flow rate ratio of NTO and MMH (O/F) close to 1.65, a fuel-rich condition [14,15]. To investigate the probable NTO/MMH impinging spray phenomena for a 5-lb$_f$ thruster, this study varied the O/F ratio from 1.0 up to 2.4.

The PLIF technique was adopted to observe the planar mass distributions in the spray fans (Fig. 2). A 1 mm $\times$ 50 mm laser sheet from a second harmonic Nd-YAG (yttrium aluminum garnet) laser (Model Lotis TII) was aligned to cross the spray fan at 10 mm downstream from the impinging point. Images of the liquid droplets containing dye (sulforhodamine 101) in the laser sheet were acquired

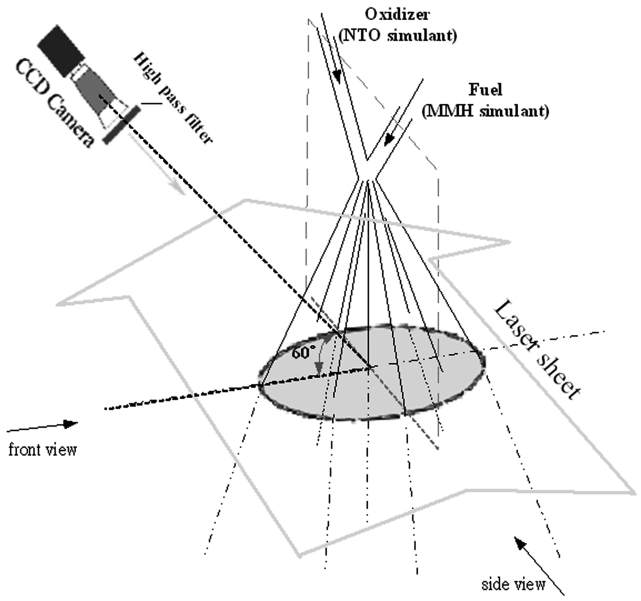

Fig. 2 The arrangement of PLIF observations.

with a pseudocolor CCD (1280 $\times$ 1024 pixels) camera. A 600 nm high-pass filter was used to eliminate the scattering light from the droplets. The average of 100 fluorescent images ($\sim$628 nm) for each experiment was recorded for analysis.

The intensity of the fluorescence is directly proportional to the amount of the excitable dye molecules. The fluorescent intensity can be described as

$$f_{x,y} = C_f' I_0(x,y) n = C_f I_0(x,y) m_{x,y} \tag{1}$$

where C_f is a collective coefficient of the optical setup, spectroscopic characteristics of dye, and temperature and pressure effects on fluorescent intensity [16]. Because the dye's concentration (grams of dye/grams of simulant) was kept constant in the preparation of all the test solutions, the local fluorescent intensities in the PLIF images would be proportional to the local liquid mass [17].

Instead of trying to determine the absolute mass distribution of liquid droplets from the intensity profile of a PLIF image, probability distribution of mass was used to describe the spray structure. Because the values of C_f and $I_0(x,y)$ were verified to have an insignificant difference across the 2-D spray images, the probability distribution of mass was determined by

$$P_{x,y} = \frac{m_{x,y}/\Delta x \Delta y}{\int_a^b \int_c^d (m_{x,y}/\Delta x \Delta y)\mathrm{d}x\mathrm{d}y} \cong \frac{f_{x,y}/\Delta x \Delta y}{\int_a^b \int_c^d (f_{x,y}/\Delta x \Delta y)\mathrm{d}x\mathrm{d}y} \tag{2}$$

where (a, b) and (c, d) were the observation ranges in x and y directions, Δx and Δy, the resolution of the observation grid was 0.24 mm. For all the 2-D probability distribution figures presented in this study, the outer contour of the constant probability is 5×10^{-4} mm^{-2} and the increment between contours is 3×10^{-3} mm^{-2}. Considering the system at steady state, the local mixture ratio was evaluated by

Table 1 Physical properties of test fluids

Test Fluid	Water, vol %	Chloroform, vol %	Methanol, vol %	Density, ρ, g/cm^3	Viscosity, μ, 10^{-3} N $\cdot$ s/m^2	Surface tension, σ, 10^{-3}N/m
MMH simulant	95	——	5	0.99	1.11	32.9[a]
NTO simulant	——	95	5	1.41	0.57	25.7
MMH				0.88	0.85	33.5
NTO				1.45	0.42	26.5
Water				1.00	0.89	71.8

[a]Surfactant added to decrease surface tension.

Table 2 The experimental conditions and results of doublet impingements with a total mass flow rate of 8.0 g/s

No.	O/F	Momentum flux ratio $m_0^* v_0/m_f^* v_f$	Jet velocity m/s	Reynolds no.	$\bar{M}$ kg/kmol	Ratio of specific heat k	E_m %	$\bar{T}$ K	Ideal C^* m/s	$\bar{C}^*$ m/s
1	1.04	0.72	39.4/56.9	32,745/15,062	17.0	1.27	77	2160	1624	1503
2	1.18	0.93	42.0/53.4	34,907/14,144	17.8	1.24	91	2450	1646	1607
3	1.43	1.37	45.5/47.6	37,869/12,615	19.0	1.22	86	2450	1664	1582
4	1.60	1.70	47.8/44.9	39,791/11,889	19.8	1.20	79	2537	1664	1582
5	1.79	2.14	49.9/41.9	41,552/11,086	20.6	1.20	77	2663	1658	1537
6	2.04	2.77	51.4/37.8	42,753/10,016	21.5	1.19	69	2602	1643	1451
7	2.22	3.30	53.5/36.1	44,514/9557	22.1	1.19	65	2482	1629	1414
8	2.39	3.81	54.1/33.9	44,995/8984	22.6	1.19	66	2483	1614	1407

Table 3 The experimental conditions and results of triplet impingements with a total mass flow rate of 8.0 g/s

No.	O/F	Momentum flux ratio $m_0^* v_0/m_f^* v_f$	Jet velocity m/s	Reynolds no.	$\bar{M}$ kg/kmol	Ratio of specific heat k	E_m %	$\bar{T}$ K	Ideal C^* m/s	$\bar{C}^*$ m/s
9	1.02	39.5/226.3	19.9/57.2	16,213/15,138	16.9	1.27	87	2224	1619	1556
10	1.19	45.7/193.3	21.0/52.8	17,454/13,991	17.8	1.24	87	2384	1648	1577
11	1.41	52.9/160.1	22.6/48.1	18,775/127,630	18.9	1.22	83	2446	1663	1564
12	1.59	58.2/137.8	23.7/44.6	19,695/118,128	19.7	1.20	86	2617	1664	1575
13	1.83	64.6/115.6	24.9/40.9	20,736/10,818	20.7	1.20	78	2605	1656	1515
14	2.29	74.6/85.2	26.8/35.1	22,297/9289	22.3	1.19	79	2658	1623	1496
15	2.38	75.7/80.4	27.0/34.1	22,457/9022	22.6	1.19	77	2628	1615	1473

Table 4 The list of the spray patternation index of doublet impingements. Case A and case B are the calculated results based on the grid resolution of 0.24 and 2 mm, respectively

No.	O/F	Momentum flux ratio, $m_0^* v_0/m_f^* v_f$	Spray patternation index (P.I.)					
			Total mass		Mass distribution of NTO		Mass distribution of MMH	
			Case A	Case B	Case A	Case B	Case A	Case B
1	1.04	0.72	102	109	99	113	107	110
2	1.18	0.93	107	104	105	113	106	107
3	1.43	1.37	101	111	105	116	102	108
4	1.60	1.70	104	113	108	115	103	114
5	1.79	2.14	111	121	113	119	102	112
6	2.04	2.77	116	123	122	128	98	104
7	2.22	3.30	118	128	126	137	104	114
8	2.39	3.81	113	127	121	132	99	115

$$R_{x,y} = \frac{P_{x,y,\mathrm{NTO}} \cdot \dot{m}_{\mathrm{NTO}}}{P_{x,y,\mathrm{MMH}} \cdot \dot{m}_{\mathrm{MMH}}} \tag{3}$$

where $P_{x,y}$ and $\dot{m}$ were the local mass distribution probability and the mass flow rate of the simulants. The spray patternation index [18] and the mixing efficiency [3] were also evaluated, with P.I. indicating the uniformity of the spray is zero for the most uniform spatial distribution. E_m defining the degree of mixing is calculated by

$$E_m = 100\left[1 - \left(\sum_a^b \sum_c^d P_{x,y} \frac{R - r_{\mathrm{sb}_{x,y}}}{R} + \sum_{a'}^{b'} \sum_{c'}^{d'} P_{x,y} \frac{R - r_{\mathrm{sa}_{x,y}}}{R-1}\right)\right] \tag{4}$$

where R is the global mixture ratio expressed as the mass flow rate ratio of oxidizer and the total flow. To evaluate the hot-firing performance, the local adiabatic flame temperatures and the local characteristic exhaust velocity were also calculated by knowing $R_{x,y}$. The average exhaust temperature and the average characteristic exhaust velocity were then determined by

$$\bar{T} = \int_a^b \int_c^d P_{x,y} \cdot T_{x,y} \mathrm{d}x\mathrm{d}y \tag{5}$$

and

$$\bar{C}^* = \int_a^b \int_c^d P_{x,y} \cdot C_{x,y}^* \mathrm{d}x\mathrm{d}y \tag{6}$$

III. Results and Discussion

The experimental conditions and results are listed in Table 2 for doublet impingements and Table 3 for triplet impingements. Contours of constant probability of total mass distributions are shown in Fig. 3 for doublet impingements, where the MMH simulant (F jet) was injected from the right and the NTO simulant (O jet) was injected from the left-hand side of the figures. At $O/F = 1.04$, the spray was shifted and weakly concaved to the left because the F jet had larger momentum. The most uniform distribution was presented at $O/F = 1.18$, where the O jet and the F jet had nearly equal momentum. When the O/F ratio was above 1.18, the distributions started shifting and concaving to the right and became more concentrated as the increase of the O/F ratio. In fact, an incomplete breakup of the O jets appeared when $O/F \geq 1.79$.

For the mass distribution of the MMH simulant (see Fig. 4), the uniformity increased with increasing O/F ratios up to 1.60. Above that O/F ratio, MMH distributions were getting more concentrated even with stronger impingement by the O jet. A possible explanation

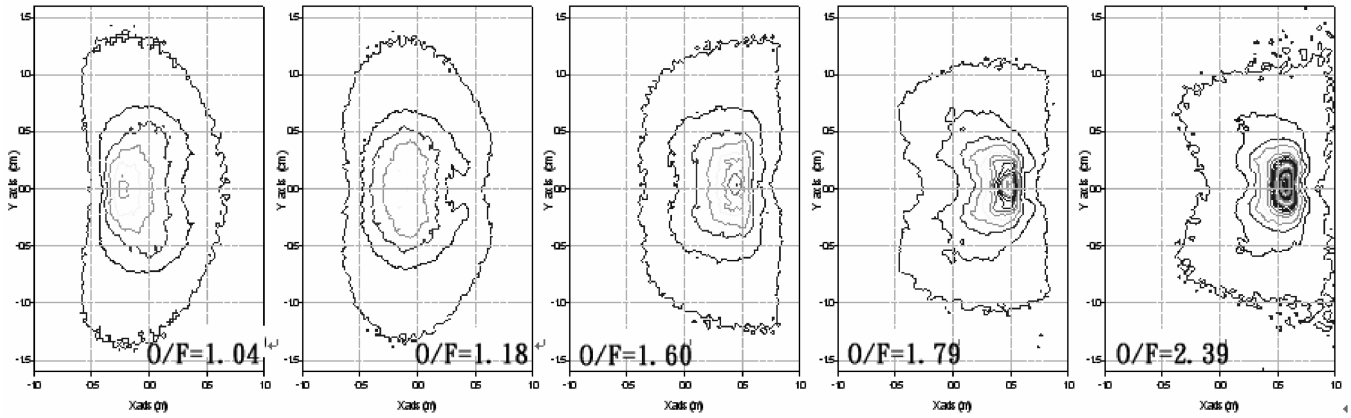

Fig. 3 The 2-D probability distributions of total mass at 10 mm from the impinging point for doublet impingements. (The outer contour of constant probability is 5×10^{-4} mm^{-2} and the increment between contours is 3×10^{-3} mm^{-2}.)

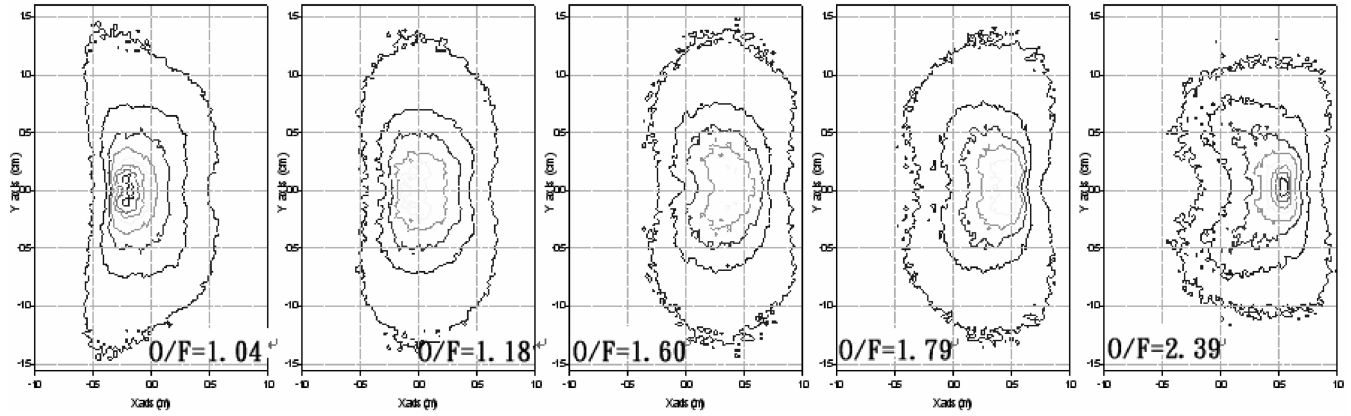

Fig. 4 The 2-D probability distributions of mass of MMH simulant at 10 mm from the impinging point for doublet impingement simulants. (The outer contour of constant probability is 5×10^{-4} mm^{-2} and the increment between contours is 3×10^{-3} mm^{-2}.)

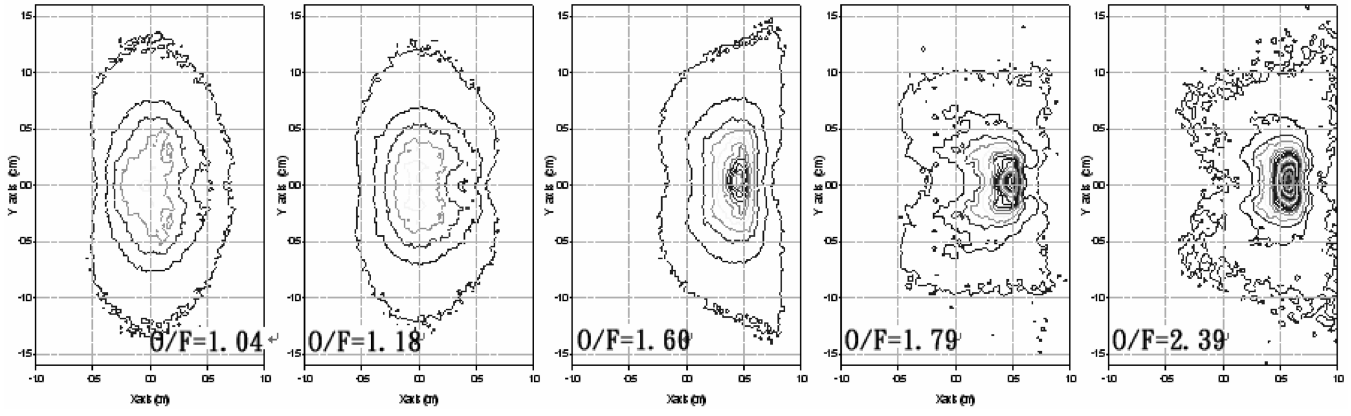

Fig. 5 The 2-D probability distributions of mass of NTO simulant at 10 mm from the impinging point for doublet impingement simulants. (The outer contour of constant probability is 5×10^{-4} mm^{-2} and the increment between contours is 3×10^{-3} mm^{-2}.)

is that F jet had small and decreasing Reynolds numbers (as low as $\sim$9000) when the O/F ratio increased from 1.60 to 2.39 (see Table 2). The weakened hydrodynamic instability at low Reynolds numbers confined the F jet to breakup. At momentum flux ratios less than 1 ($O/F = 1.04$), the O jet broke up more even than the F jet for having a smaller surface tension (see Figs. 4 and 5). The results revealed that surface tension, momentum flux, and Reynolds number were strongly affecting the breakup of the impinging jets.

For triplet impingements, the center jet was the F jet impinging by two O jets at ± 30 deg. Basically, the atomization and dispersion of liquids was mainly from the impingement of the two side jets. That is, increasing the O/F ratio enhanced the quality of spray. The triplet-impinging sprays had more symmetric and uniform distribution in a smaller area compared to that of the doublet impingements. From the probability distributions of the total mass as shown in Fig. 6, the uniformity of the distribution increased with the O/F ratio. The phenomenon is very similar to that of like-doublet impingements with equal jet velocities. At high enough momentum of the side jets to completely disintegrate the center jet, the penetration of the atomized O jets increased with O/F ratios. This effect is confirmed by the wider distributed spray at the O/F ratio of 2.2 compared to that at O/F of 1.6 as shown in Figs. 6 and 8. At the same time, the droplets of the F jet were dispersed by the penetrating NTO droplets, but their distribution was dimly improved with the increase of the O/F ratio (see Fig. 7).

The calculated spray patternation indexes based on two grid resolutions (0.24 and 2.0 mm) of doublet impingements are listed in Table 4. Because the numbers of the effective grids (liquid existed in

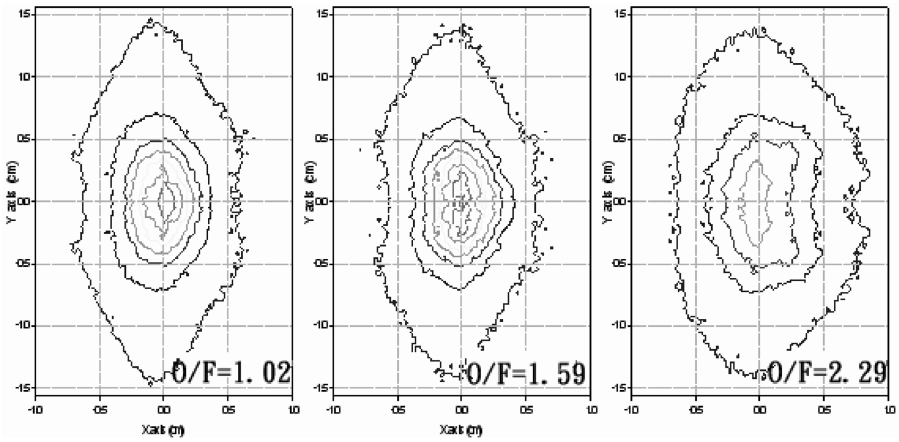

Fig. 6 The 2-D probability distributions of total mass at 10 mm from the impinging point for triplet impingements. (The outer contour of constant probability is 5×10^{-4} mm^{-2} and the increment between contours is 3×10^{-3} mm^{-2}.)

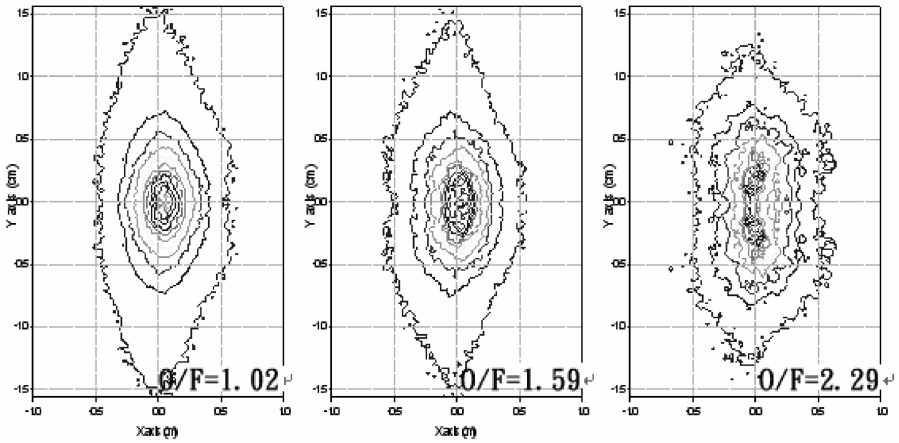

Fig. 7 The 2-D probability distributions of mass of MMH simulant at 10 mm from the impinging point for triplet impingement simulants. (The outer contour of constant probability is 5×10^{-4} mm^{-2} and the increment between contours is 3×10^{-3} mm^{-2}.)

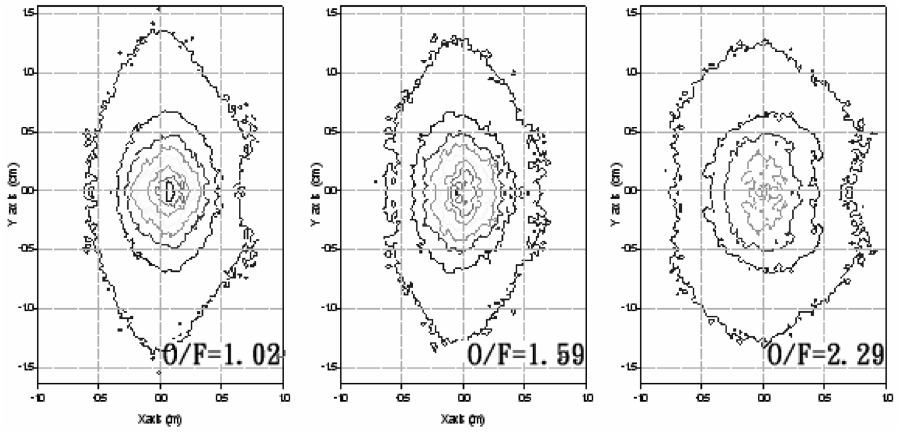

Fig. 8 The 2-D probability distributions of mass of NTO simulant at 10 mm from the impinging point for triplet impingement simulants. (The outer contour of constant probability is 5×10^{-4} mm^{-2} and the increment between contours is 3×10^{-3} mm^{-2}.)

the grid region) were different with different grid resolutions, the calculated values of the P.I. of the two cases were not the same as expected. Besides the two extreme conditions ($O/F = 1.04$ and 2.39) where a larger number of empty grids were observed, the profiles of the P.I. of both grid resolutions matched the observations from the figures of the mass probability distributions. And, the P.I. of 2.0 mm resolution with a similar resolution of the conventional mechanical patternator were predicted as the most uniform mass distribution at $O/F = 1.18$ (momentum flux ratiomomentum flux ratio = 0.93).

Mixing phenomena were also analyzed by looking at the local mixture ratio distributions of doublet impingements (Fig. 9). At $O/F = 1.04$, the concentrated MMH droplets penetrated the dispersed NTO droplets and produced a relatively NTO-rich region (light gray area) stationed at the right-hand side of the MMH rich region (dark gray area). A more complete breakup of both jets showed at $O/F = 1.18$, where mutual penetration and a better mixing occurred. As the O/F ratio reached 1.60, a strong and concentrated NTO spray penetrated through the well-dispersed MMH spray, which resulted in a MMH rich region distributed at the

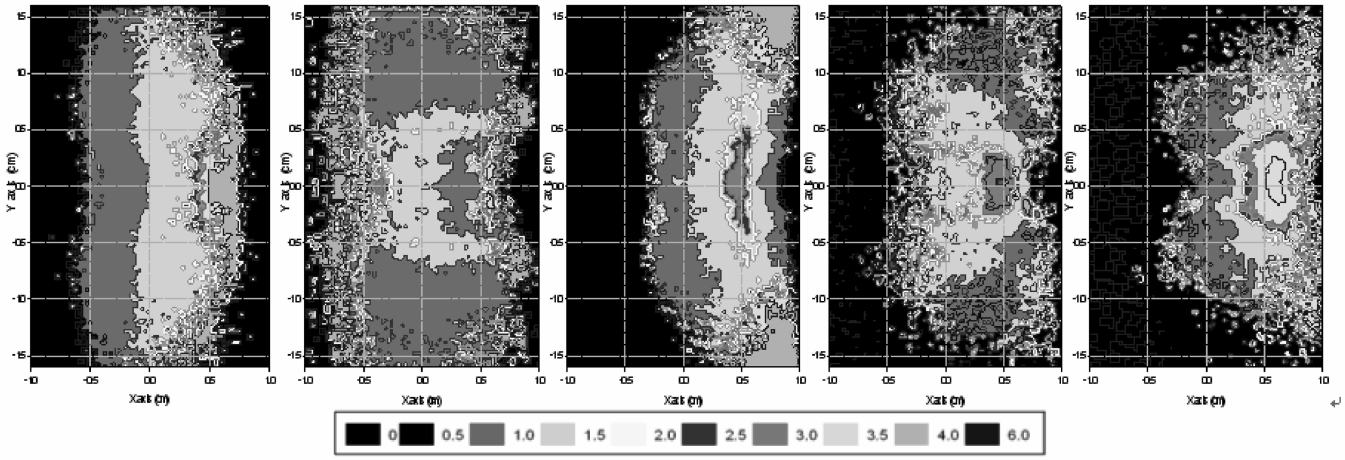

Fig. 9 The 2-D local mixing ratio distributions of doublet impingements. The O/F ratios are 1.0, 1.2, 1.6, 1.8, and 2.4 from left to right, respectively.

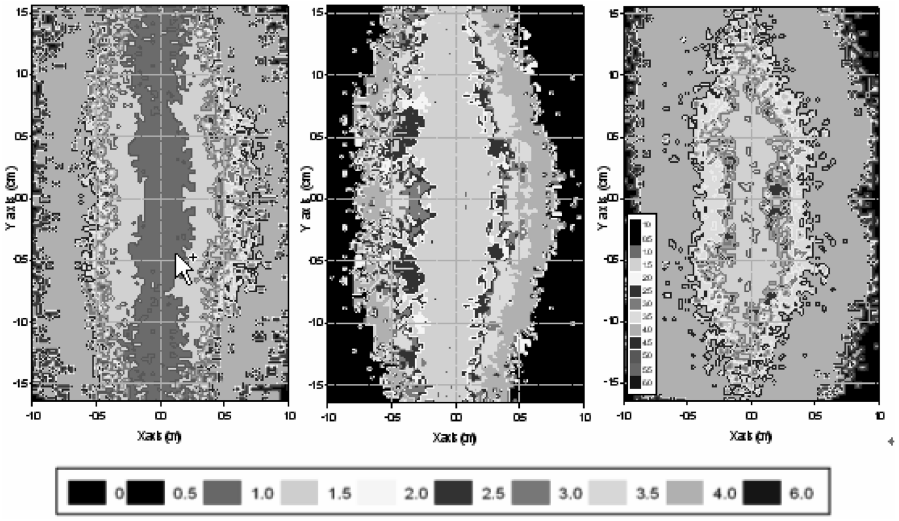

Fig. 10 The 2-D local mixing ratio distributions of triplet impingements. The O/F ratios are 1.0, 1.6, and 2.2 from left to right, respectively.

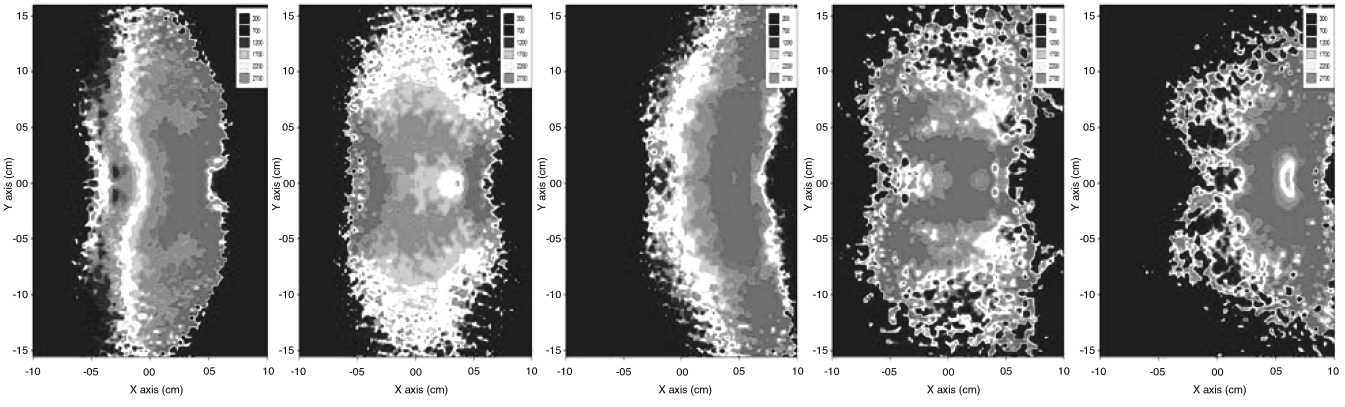

Fig. 11 The 2-D local mixing ratio distributions of triplet impingements. The O/F ratios are 1.0, 1.6, and 2.2 from left to right, respectively.

left of the total spray. At even higher O/F ratios, the NTO spray became more and more concentrated as shown in the figures.

For the mixing of triplet impingement at the O/F ratio of unity (see Fig. 10), the O jets were not able to effectively disintegrate and disperse the dense center MMH liquid, which resulted in a poor mixing and leaving a MMH rich region in the spray core. As the momentum of both O jets increased at $O/F = 1.6$, a better breakup of the F jet occurred and a more uniform mixing appeared in the spray core. Further increase of the O/F ratio effectively enhanced the NTO penetration, however, the dispersion of MMH droplets near the center was not improved. The mixture ratios near the centerline became even richer than that had shown in the case of $O/F = 1.6$. In all the O/F ratios studied for triplet impingements, the spray core was surrounded by NTO-rich droplets.

The calculated mixing efficiencies using Eq. (4) are listed separately in Tables 2 and 3. The results showed that the spray had the optimum mixing efficiency at the unity of momentum ratio ($O/F = 1.2$) of doublet impingement, which is consistent with the observation by Rupe [4]. The values of E_m of triplet impingements were less sensitive to momentum flux ratio and showed a better

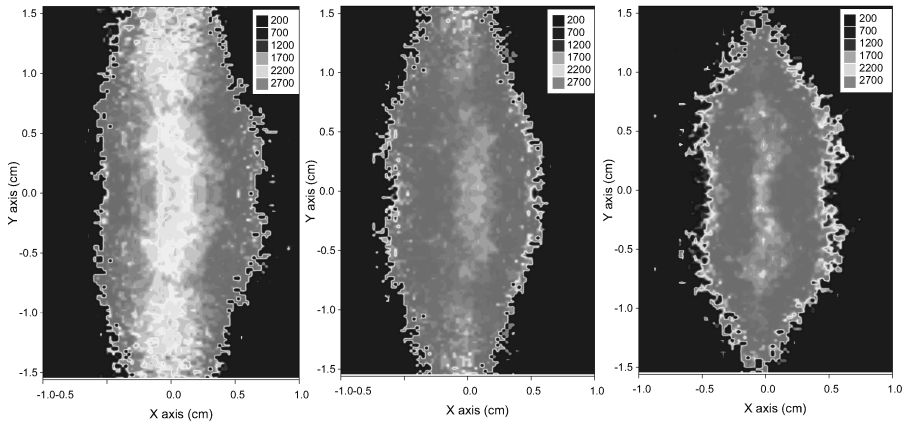

Fig. 12 The 2-D flame temperature distributions of triplet impingements. The O/F ratios are 1.0, 1.6, and 2.2 from left to right, respectively.

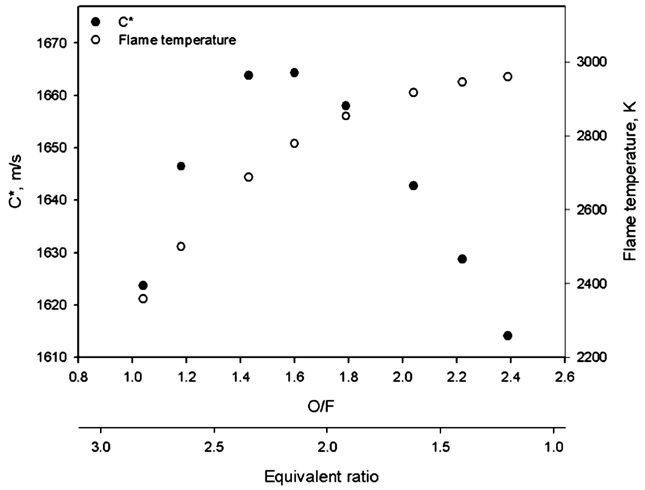

Fig. 13 The profiles of the ideal characteristic exhaust velocities and the adiabatic flame temperatures with respect to O/F ratio variation. The ideal characteristic exhaust velocities calculated based on perfect mixing.

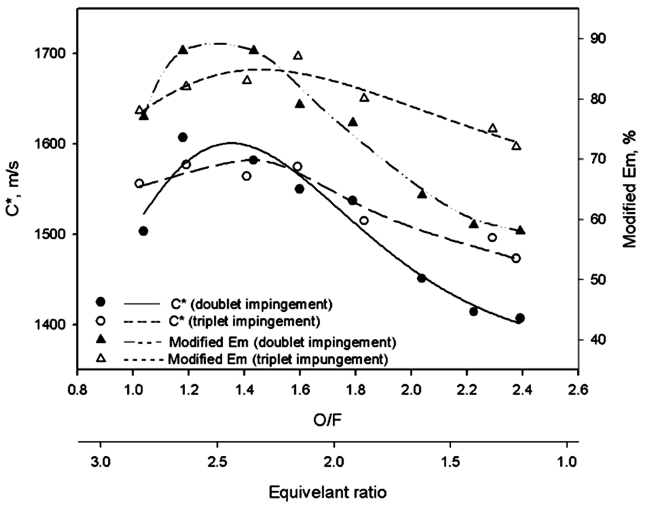

Fig. 14 The profiles of the calculated average characteristic exhaust velocities and the modified efficiencies with respect to O/F ratio variation.

mixing effect than doublet impingements at higher O/F ratio conditions.

Flame temperature distributions of several O/F ratios of doublet impingements are shown in Fig. 11. Although a better mixing occurred at $O/F = 1.18$, the temperatures distributed in the spray core were relatively low (~2550 K). Higher temperatures (~2880 K) in the spray core were observed at $O/F = 1.60$–1.79. For $O/F > 1.79$, a NTO-rich low temperature area coexisted in the core lowering the average exhaust temperature ($\bar{T}$). For triplet impingements, low flame temperatures ($T \sim 2100$ K) were clearly shown in the spray core at $O/F = 1$ (Fig. 12). Higher flame temperatures ($T \sim 2650$ K) appeared at the O/F ratio above 1.79. The average flame temperatures calculated by Eq. (5) are also listed in Tables 2 and 3. It shows that the triplet-impinging arrangement had a superior thermal performance at the high O/F ratio than that of the doublet impinging arrangement.

The theoretical characteristic exhaust velocity deduced from the isentropic steady flow process is used to predict the combustion efficiency of propellants [19]. The values of C^* were also evaluated in this study. The required parameters in the evaluations such as the ratio of k and $\bar{M}$ were determined from the equilibrium composition of the combusted gas calculated by CEC86. The data are listed in Tables 2 and 3 and show that the average molecular weight increased with the increasing O/F ratio. Figure 13 shows the profiles of flame temperature and C^* assuming perfect mixing of NTO/MMH. An optimum C^* exists because of the collective effects of k, $\bar{M}$, and T. The O/F ratio corresponding to the optimum C^* (O/F_{opt}) can be treated as a property of a specific propellant system. For the NTO/MMH system, $O/F_{\text{opt}} \approx 1.5$ with the optimum $C^* \approx 1664$ m/s. $\bar{C}^*$ of the experiments were calculated and are listed and plotted in Tables 2 and 3, and Fig. 14. The optimum $\bar{C}^*$ was located at the $O/F = 1.18$ for the doublet impingements and was located in the $O/F = 1.19$–1.59 for the triplet impingements. These results implied that the mixing condition corresponding to the optimum $\bar{C}^*$ should have the highest probability of local mixture ratio ($R_{x,y}$) lying around 1.5. This argument was verified by replacing R in Eq. (4) by O/F_{opt} and calculating the modified E_m, where the modified E_m represents a measurement of the "closeness" of $R_{x,y}$ to O/F_{opt}. The results are also plotted in Fig. 14, which showed that the optimum modified E_m occurred at $O/F = 1.18$ for doublet impingements and at 1.59 for triplet impingements and is consistent with the O/F ratios for the optimum $\bar{C}^*$s.

IV. Conclusion

In this simulation of the impinging mixing of a 5-lb_f MMH/NTO rocket, the overall analysis shows that surface tension, momentum flux, and Reynolds number of the impinging jet have strong effects

on the jet's breakup and mass distribution. These observations are consistent with the instability theory discussed by previous researchers [20]. In the O/F ratios studied, the triplet impingement is superior in symmetry and uniformity of the spray than that of the doublet impingement. With the detailed information provided by the optical technique, this study demonstrated that the operation condition to have the optimum $\bar{C}^*$ can be predicted using O/F_{opt} and the calculation of the modified E_m. For the operation of a 5-lb_f NTO/MMH rocket, the optimum $\bar{C}^*$ occurred at $O/F = 1.18$ with doublet impingements, which happened corresponding to a condition that closed to unity momentum flux ratio and the best mixing. Although continued research is required to verify the predicted results by hot-firing experiments, this study showed that the PLIF technique coupled with a simple statistical analysis can be used for detailed analysis of small-size impinging sprays.

References

[1] Lecourt, R., and Foucaud, R., "Hypergolic Propellant Burning Spray Visualization by Laser Sheet Method: Application to Droplet Size and Liquid Concentration Measurements," Experimental and Numerical Flow Visualization, *Proceedings of the 1993 ASME Winter Annual Meeting*, edited by B. Khalighi et al., Vol. 172, American Society of Mechanical Engineers, New York, 1993, pp. 173–181.

[2] Seamans, T. F., and Vanpee, M., "Development of a Fundamental Model of Hypergolic Ignition in Space-Ambient Engines," *AIAA Journal*, Vol. 5, No. 9, Sept. 1967, pp. 1616–1624.

[3] Rupe, J. H., "The Liquid Phase Mixing of A Pair of Impinging Streams," Jet Propulsion Lab., JPL Progress Rept. 20-195, California Institute of Technology, Pasadena, CA, 1953.

[4] Rupe, J. H., "A Correlation Between the Dynamic Properties of a Pair of Impinging Streams and the Uniformity of Mixture Ratio Distribution in the Resulting Spray," Jet Propulsion Lab., JPL Progress Rept. 20-209, California Institute of Technology, Pasadena, CA, 1956.

[5] Won, Y. D., Cho, Y. H., Lee, S. W., and Yoon, W. S., "Effect of Momentum Ratio on the Mixing Performance of Unlike Split Triplet Injectors," *Journal of Propulsion and Power*, Vol. 18, No. 4, July–Aug. 2002, pp. 847–854.

[6] Riebling, R. W., "Criteria for Optimum Propellant Mixing in Impinging-Jet Injector Elements," *Journal of Spacecraft and Rockets*, Vol. 4, No. 6, June 1967, pp. 817–819.

[7] Ashgriz, N., Brocklehurst, W., and Tally, D., "Mixing Mechanism in a Pair of Impinging Jets," *Journal of Propulsion and Power*, Vol. 17, No. 3, May–June 2001, pp. 736–749.

[8] McHale, R. M., Nurick, W. H., and Clapp, S. D., "Injector Design Criteria Using Noncircular Orifice Geometry," *Journal of Spacecraft and Rockets*, Vol. 8, No. 4, April 1971, pp. 408–410.

[9] Nurick, W. H., and Clapp, S. D., "An Experimental Technique for Measurement of Injector Spray Mixing," *Journal of Spacecraft and Rockets*, Vol. 6, No. 11, Nov. 1969, pp. 1312–1314.

[10] Koh, H., Kim, D., and Yoon, Y., "Correction of Attenuation Effects in Dense Sprays Using Planar Imaging Technique," *Proceedings of the 10th International Symposium on Flow Visualization*, F0188, 2002.

[11] Jung, K., Lim, B., Yoon, Y., and Koo, J.-Y., "Comparison of Mixing Characteristics of Unlike Triplet Injectors Using Optical Patternator," *Journal of Propulsion and Power*, Vol. 21, No. 3, May–June 2005, pp. 442–449.

[12] Yuan, T., and Chen, C., "Observations of the Spray Phenomena of Unlike-Doublet Impinging Jets," *Proceedings of the 11th International Symposium on Flow Visualization*, F064, 2004.

[13] Sankar, S. V., Maher, K. E., Robart, D. M., and Bachalo, W. D., "Rapid Characterization of Fuel Atomizers Using an Optical Patternator," *Journal of Engineering for Gas Turbines and Power*, Vol. 121, July 1999, pp. 409–414.

[14] Schindler, R. C., and Schoenman, L., "Development of a Five-Pound Thrust Bipropellant Engine," *Journal of Spacecraft and Rockets*, Vol. 13, No. 7, July 1976, pp. 435–442.

[15] Stechman, R. C., and Smith, J. A., "Monomethyl Hydrazine vs. Hydrazine Fuels: Test Results Using Flight Qualified 100 lb_f and 5 lb_f Bipropellant Engine Configurations," AIAA Paper 83-1257, 1983.

[16] Eckbreth, A. C., *Laser Diagnostics for Combustion Temperature and Species*, Gordon and Breach, New York, 1996, p. 390.

[17] Talley, D. G., Verdieck, J. F., Lee, S. W., Mcdonell, V. G., and Samuelsen, G. S., "Accounting for Laser Sheet Extinction in Applying PLLIF to Sprays," AIAA Paper 96-0469, 1996.

[18] Tate, R. W., "Spray Patternation," *Industrial and Engineering Chemistry*, Vol. 52, No. 10, Oct. 1960, pp. 49A–53A.

[19] Sutton, G. P., *Rocket Propulsion Elements*, Wiley, New York, 1992.

[20] Dombrowski, N., and Hopper, P. G., "A Study if the Sprays Formed by Impinging Jets in Laminar and Turbulent Flow," *Journal of Fluid Mechanics*, Vol. 18, No. 3, 1964, pp. 392–400.

R. Lucht
Associate Editor